On the feasibility of small-data learning in simulation-driven engineering tasks with known mechanisms and effective data representations

Anonymous Author(s)
Affiliation
Address
email

Abstract

The application of machine learning (ML) in scientific tasks is increasing, especially ML in simulation-driven engineering tasks. While previous studies were mostly model-centric and required large-data learning, recent studies start to pay attention to data-centric AI and are investigating small-data learning with effective structured representations, which is significant for industrial application. This article provides a theoretical discussion for the feasibility of small-data learning with structured representations, which is then verified through the surrogate modelling of hot stamping simulations. Future directions are also discussed.

1 Introduction

In the past decade, ML, particularly deep learning, has been successfully applied to general Artificial Intelligence (AI) tasks, including object detection [1], semantic segmentation [2], and image generation [3]. Recently, ML is being extended to scientific tasks, which can be broadly classified into mechanism-unknown tasks and mechanism-known tasks, as shown in Figure 1. In mechanism-unknown tasks, ML can be applied to mathematically formulating the mechanisms, such as ML-assisted material modelling [4][5], or explorative discovery with unknown or partly-unknown mechanisms, such as discovering new materials [6] or drugs [7]; in mechanism-known tasks, also known as simulation-driven engineering tasks, the mechanisms have been mathematically formulated and integrated with simulation tools, such as finite element analysis (FEA), while ML is mainly applied to surrogate-based optimisation [8]. A frequent observation is that the application of ML is more convenient and practical in simulation-driven engineering tasks than in mechanism-unknown tasks, since multi-scale simulation tools can generate data containing comprehensive info, such as physical fields, that are difficult to obtain in experiments. Therefore, this article mainly focuses on ML-assisted surrogate-based optimisation in simulation-driven engineering tasks.

In ML-assisted surrogate-based optimisation, while some studies replaced classical optimisers with ML, such as reinforcement learning [9], most efforts have been devoted to improving the accuracy, generalisability, and interpretability of surrogate models. Current ML with scalar representations of both inputs and outputs, such as Kriging models [10][11], has been widely deployed. However, these models are only suitable for low-dimension, single-parameterisation, scalar-output use cases, while it is difficult to integrate data from multiple parameterisations or reuse historical data. To improve the performance of ML-assisted surrogate models, including their flexibility, accuracy and generalisability, recent studies have intensively investigated ML with structured representations, such as fields [12] and graphs [13]. ML with structured representations was initially practiced in computational fluid dynamics (CFD), since Eulerian meshing, which is popular in most CFD tasks, can be conveniently integrated with convolutional neural networks (CNN). Guo, Xu. et al. represented 2D or 3D geometries using signed distance functions (SDF) [14]. Based on the SDF field representations, a

Submitted to NeurIPS 2021 AI for Science Workshop.

CNN was trained to predict the full fields of 2D or 3D non-uniform steady laminar flow. ML with structured representations, which integrates advanced architectures such as recurrent neural networks (RNNs) and generative adversarial networks (GANs), has been applied to more complex CFD cases, including temporal prediction [15][16] and inverse design [17][18]. Based on the success in CFD cases, ML with structured representations has been extended to difficult use cases where non-Eulerian meshing is applied, including solid mechanics [19], structured optimisation [20][21], manufacturing [22][23][24], and meta-material design [25][26].

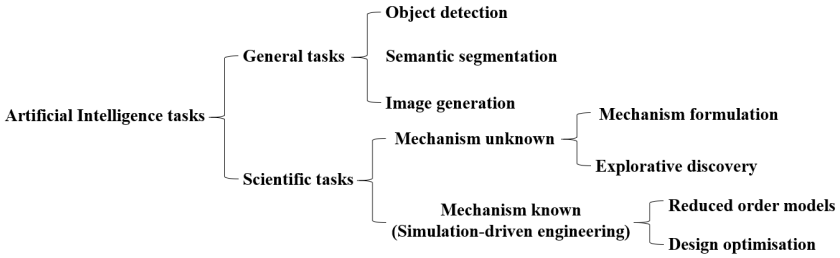

Figure 1: Classification of AI tasks.

The ML-assisted surrogate models discussed above mainly employed full field-based representations, which significantly improved the overall performance of surrogate models. The previous studies discussed above mostly pursued universally-generalised models, large-data training, and high-resolution full-field representations. Recent studies have started to investigate more effective structured representations, such as implicit shape parameterisation [27][28][29][30][31][32] and graphs [12][38]; surrogate models are trained on datasets with task-specific sizes [33][34][35]. Despite the emerging trend discussed above, only a few studies attemped to investigate the feasibility of small-data learning and the benefits of effective representations: Cao et al. showed that non-parametric input representation using graph neural network (GNN) and field-based output representation significantly improved the performance of surrogate models [12]; Li et al. significantly reduced the dataset size, which was acceptable for industrial practice and significantly facilitated multi-query optimisation, using wing mode representations [30][33].

In this article, the feasibility of small-data learning and the benefits of effective representations will be investigated based on the surrogate modelling of a case with application to hot stamping. In section 2, the feasibility and benefits will be discussed based on theoretical considerations. In section 3, a hot stamping case will be presented for verification. In section 4, current studies will be summarised and future directions will be pointed out.

2 Theoretical discussion

In this section, the feasibility of small-data learning in simulation-driven engineering tasks will be theoretically discussed by comparing these tasks with general tasks, and the benefits and criteria of effective representations will be discussed. The feasibility of small-data learning in mechanism-unknown tasks remains an open research question due to the lack of physical mechanisms, which is out of the scope of this article and requires further study.

2.1 The feasibility of small-data learning in simulation-driven engineering tasks

The definition of small-data and the required dataset size largely depends on specific tasks. In general tasks, datasets that containing millions of data samples are required to ensure the performance of ML, such as ImageNet and Open Images. However, simulation-driven engineering tasks are expected to require much less data thanks to the following three attributes:

- From the input side, the design variables and corresponding domain in simulation-driven engineering tasks can be explicitly defined. For instance, in a stiffness-driven shape optimisation task, the shape can be completely defined by a set of variables and uniformly generated using sampling strategies, such as Latin hypercube [37]. This ensures an effective coverage of the design space. However, in general tasks such as a multi-classification, it is nearly impossible to define the features of a certain class using explicit variables, not to

mention sampling strategies. In this case, large data is required to better cover the design space of general tasks, while mode collapse still occurs.

- From the output side, in a multi-classification task, laborious labelling work is required in supervised and semi-supervised learning. Furthermore, the labels are usually not embedded in a mathematical metric space: it is nonsense to say 'cat'>'dog' on the math. This might lead to highly nonlinear and complicated input-output mapping relationships. However, the outputs of simulation-driven engineering tasks are mostly fields with inherent mechanism driven patterns. Labelling work is rarely required while the outputs are in nature mathematically comparable.
- Data in simulation-driven engineering tasks usually has a higher signal-to-noise ratio (SNR). To clarify, a cat in a multi-classification task may be classed under diverse headings because the image contains features such as eyes, irrelevant objects and background. This has a negative effect on data quality and SNR. However, data in simulation-driven engineering tasks, as long as the simulation model is verified and uncertainty is estimated, contains little irrelevant information.

These advantageous attributes lead to smoother input-output mapping relationships and significantly reduces the data requirement in simulation-driven engineering.

2.2 The benefits and criteria of effective data representations

Besides the natural attributes discussed above, proper representations are required to reduce dataset sizes and improve the performance of surrogate models. Based on a case with application to stiffened panel optimisation, Hao et al. demonstrated that field-based input shapes preserved the topological information, compared with parametric representations [13]. To clarify, a shape usually consists of multiple inter connected features, such as rounded corners, while the interconnection relationship is lost if the shape is represented merely by the scalar feature parameters, such as radius. Based on a cold forming case, Zhou et al. demonstrated that field-based output physical fields preserved the data structure of physical fields compared with scalar performance indicators [36]. For example, multiple thinning fields that have the same maximum thinning might differ in their locations, peak number, and patterns. Overall, field-based representations have shown remarkable advantages over conventional scalar representations in academia [12][13][33][36] and industry [38][40].

3 Case study: A field-based Artificial Intelligence empowered surrogate model for a hot-stamped ultrahigh-strength-steel (UHSS) B-pillar

Small-data learning, which has been theoretically discussed in section 2, is verified based on the surrogate model of a hot stamped B-pillar used in automotive applications. The simulation setup in PAM-STAMP is shown in Figure 2, while the simulation model was experimentally verified [39].

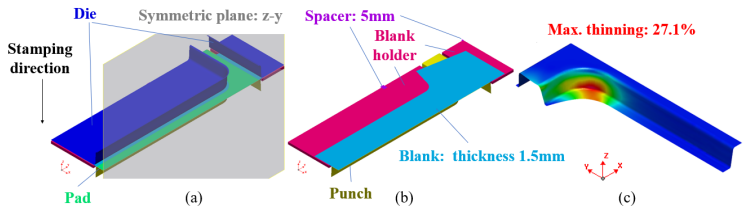

Figure 2: (a) Simulation model setup in PAM-STAMP (b) Initial blank (same model as (a) while hiding die, pad and symmetric) (c) Predicted thinning field (A key manufacturing quality indicator).

3.1 Dataset and surrogate model setup

The surrogate model predicted the full blank thinning fields, which was mapped on the 2D initial blank configuration, given the 2D images of die and blank. The design variables and domain are demonstrated in Figure 3. A training set sized 64, which could be regarded as small-data, and a validation set sized 256 were sampled from the design domain in Figure 3(b) using Latin hypercube

(LHS). Two samples in the 64-size training set and nine in the 256-size validation set had excessive thinning due to small draft angles (<1.2°) or large height (>65mm). The FEA ground truth thinning fields of these samples were not reliable due to numerical errors when excessive thinning occurred. Since this study was not discussing failure and corresponding representations, these samples were removed, which led to a 62-size training set and a 247-size validation set. The surrogate model

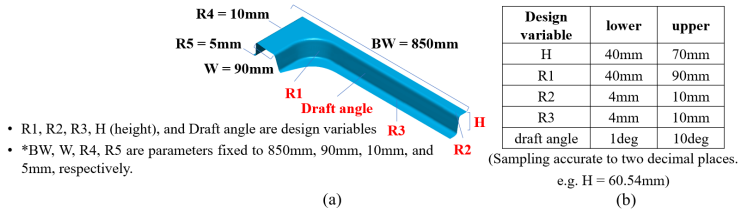

Design variable	lower	upper
H	40mm	70mm
R1	40mm	90mm
R2	4mm	10mm
R3	4mm	10mm
draft angle	1deg	10deg

Figure 3: (a) Design variables set up (b) Design domain.

was adapted based on a verified backbone architecture, namely Res-SE-U-Net that is comprised of residual modules, squeeze-excitation modules, and skip connections [19][21][36]. The details of Res-SE-U-Net were discussed in [36]. For comparison, a Gaussian process (GP) model with scalar inputs (design variables) and outputs (maximum thinning) was developed using Python/sklearn [13].

3.2 Results and discussion

Based on the 62-size training set, Res-SE-U-Net model was trained by adopting mean square error (MSE) and GP model was fitted with optimised hyperparameters. Both models were validated on the 247-size validation set. As shown in Figure 4(a)(b), the violin plot of maximum thinning predicted by Res-SE-U-Net has a better consistency with the ground truth than that predicted by GP. For Res-SE-U-Net, the average absolute relative error of the maximum thinning (AREMT)

$$ARMET = |(ML\,prediction - FEA\,ground\,truth)/FEA\,ground\,truth| \times 100\% \quad (1)$$

was 3.77%, and 82.6% samples (204/247) had AREMT below 6%. For GP, the average AREMT was 5.80%, while only 51.4% samples had AREMT below 6%. In conclusion, Res-SE-U-Net trained on small data accurately and reliably predicted scalar maximum thinning even though maximum thinning was not explicitly included in MSE loss. A potential reason is that Res-SE-U-Net predicted the full thinning field that contained intrinsic physics, as shown in Figure 4(c). Predicting full fields also provides more guiding information to engineers.

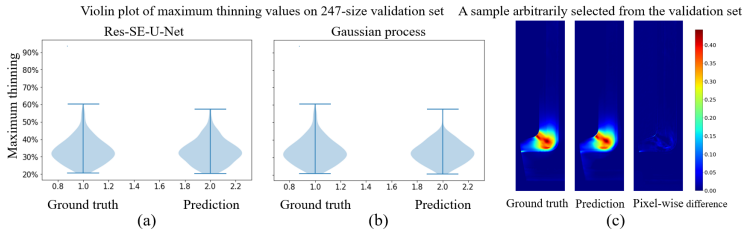

Figure 4: (a) Violin plot of maximum thinning predicted by Res-SE-U-Net (b) Violin plot of maximum thinning predicted by Gaussian process (c) Thinning fields of a validation sample.

4 Summary and future directions

In this study, small-data learning using field-based representations in simulation-driven engineering tasks was investigated and verified. The advantageous attributes that enable small-data learning were discussed in comparision with general tasks. In the case study, Res-SE-U-Net outperformed GP by leveraging the intrinsic physics in full thinning fields.

More studies on data-centric approaches in AI for science and engineering are expected in the future. Effective representations will be investigated. For example, a graph representation is preferred in a truss optimisation case since the truss contains only nodes and links [38]. Besides, active sampling, transfer learning, and physics-informed losses are promising to further facilitate small-data learning.

References

[1] Krizhevsky, A., Sutskever, I., & Hinton, G. E. (2012) ImageNet classification with deep convolutional neural networks. *Advances in neural information processing systems, 25*: pp. 1097–1105.

[2] Jégou, S., Drozdzal, M., Vazquez, D., Romero, A., & Bengio, Y. (2017) The one hundred layers tiramisu: Fully convolutional densenets for semantic segmentation. *In Proceedings of the IEEE conference on computer vision and pattern recognition workshops*, pp. 11–19.

[3] Goodfellow, I., Pouget-Abadie, J., Mirza, M., Xu, B., Warde-Farley, D., Ozair, S., Courville, A., & Bengio, Y. (2014) Generative adversarial nets. *Advances in neural information processing systems, 27*.

[4] Diamantopoulou, M., Karathanasopoulos, N., & Mohr, D. (2021) Stress-strain response of polymers made through two-photon lithography: micro-scale experiments and neural network modeling. *Additive Manufacturing*, pp. 102266.

[5] Saha, S., Gan, Z., Cheng, L., Gao, J., Kafka, O. L., Xie, X., Li, H., Tajdari, M., Kim, H. A., & Liu, W. K. (2021) Hierarchical deep learning neural networks (HiDeNN): An artificial intelligence (AI) framework for computational science and engineering. *Computer Methods in Applied Mechanics and Engineering, 373*: pp. 113452.

[6] Chen, C., & Gu, G. X. (2019) Machine learning for composite materials. *MRS Communications 9, no.2*: pp. 556-566.

[7] Elbadawi, M., Gaisford, S., & Basit, A. W. (2021) Advanced machine-learning techniques in drug discovery. *Drug Discovery Today 26, no.3*: pp. 769-777.

[8] Li, J., & Zhang, M. (2021) Data-based approach for wing shape design optimization. *Aerospace Science and Technology, 112*: pp. 106639.

[9] Sun, H., & Ma, L. (2020) Generative design by using exploration approaches of reinforcement learning in density-based structural topology optimisation. *Designs 4, no.2*: 10.

[10] Gao, F., Ren, S., Lin, C., Bai, Y., & Wang, W. (2018) Metamodel-based multi-objective reliable optimisation for front structure of electric vehicle. *Automotive Innovation 1, no.2*: pp. 131-139.

[11] Tao, S., van Beek, A., Apley, D. W., & Chen, W. (2021) Multi-model Bayesian optimisation for simulation-based design. *ASME.J.Mech.Des. 143, no.11*: pp. 111701.

[12] Cao, J., Li, Q., Xu, L., Yang, R., & Dai, Y. (2021) Non-parametric surrogate model method based on machine learning. *preprint*.

[13] Hao, P. Liu, D., Zhang, K., Yuan, Y., Wang, B., Li, G., & Zhang, X. (2021) Intelligent layout design of curvilinearly stiffened panels via deep learning-based method. *Materials & Design 197*: pp. 109180.

[14] Guo, X., Li, W., & Iorio, F. (2016) Convolutional neural networks for steady flow approximation. *In Proceedings of the 22nd ACM SIGKDD international conference on knowledge discovery and data mining*: pp. 481-490.

[15] Thuereym, N., Weiβenow, K., Prantl, L., & Hu, X. (2020) Deep learning methods for Reynolds-Averaged Navier-Stokes simulations of airfoil flows. *AIAA JOURNAL 58, no.1*: pp. 25-36.

[16] Lee, S., & You, D. (2019) Data-driven prediction of unsteady flow over a circular cylinder using deep learning. *J. Fluids. Mech. 879*: pp. 217-254.

[17] Sekar, V., Zhang, M., Shu, C., & Khoo, B. C. (2019) Inverse design of airfoil using a deep convolutional neural network. *AIAA JOURNAL 57, no.3*: pp. 993-1003.

[18] Wang, Z., Xiao, D., Fang, F., Govindan, R., Pain, C. C., & Guo, Y. (2018) Model identification of reduced order fluid dynamics systems using deep learning. *International Journal for Numerical Methods in Fluids 86, no.4*: pp. 255-268.

[19] Nie, Z., Jiang, H., & Kara, L. B. (2019) Stress field prediction in cantilevered structures using convolutional neural networks. *In International Design Engineering Technical Conferences and Computers and Information in Engineering Conference 20, no.1*: pp. 011002.

[20] Oh, S., Jung, Y., Kim, S., Lee, I., & Kang, N. (2019) Deep generative design: Integration of topology optimisation and generative models. *Journal of Mechanical Design 141, no.11*.

[21] Nie, Z., Lin, T., Jiang, H., & Kara, L. B. (2021) TopologyGAN: Topology optimisation using generative adversarial networks based on physical fields over the initial domain. *ASME. J. Mech. Des. 143, no.3*: pp. 031715.

[22] Zimmerling, C., Trippe, D., Fengler, B., & Kärger, L. (2019) An approach for rapid prediction of textile draping results for variable composite component geometries using deep neural networks. *In AIP Conference Proceedings 2113, no.1*: pp. 020007.

[23] Zimmerling, C., Poppe, C., & Kärger, L. (2019) Virtual product development using simulation methods and AI. *Lightweight Design worldwide 12, no.6*: pp. 12-19.

[24] Zimmerling, C., Poppe, C., & Kärger, L. (2020) Estimating optimum process parameters in textile draping of variable part geometries-A reinforcement learning approach. *Procedia Manufacturing 47*: pp. 847-854.

[25] Xue, T., Wallin, T. J., Menguc, Y., Adriaenssens, S., & Chiaramonte, M. (2020) Machine learning generative models fo automatic design of multi-material 3D printed composite solids. *Extreme Mechanics Letters 41*: pp. 100992.

[26] Wang, L., Chan, Y., Ahmed, F., Liu, Z., Zhu, P., & Chen, W. (2020) Deep generative modeling for mechanistic-based learning and design of metamaterial systems. *Comput. Methods Appl. Mech. Engrg. 372*: pp. 113377.

[27] Park, J. J., Florence, P., Straub, J., Newcombe, R., & Lovegrove, S. (2019) Deepsdf: Learning continuous signed distance functions for shape representation. *In Proceedings of the IEEE/CVF Conference on Computer Vision and Pattern Recognition*: pp. 165-174.

[28] Remelli, E., Lukoianov, A., Richter, S. R., Guillard, B., Bagautdinov, T., Baque, P., & Fua, P. (2020) MeshSDF: Differentiable iso-surface extraction. *34th Conference on Neural Information Processing Systems (NeurIPS 2020)*

[29] Guillard, B., Remelli, E., Lukoianov, A., Richter, S., Bagautdinov, T., & Baque, P. (2021) DeepMesh: Differentiable iso-surface extraction. *arXiv:2106.11795v1*.

[30] Li, J., & Zhang, M. (2021) Adjoint-free aerodynamic shape optimisation of the common research model wing. *AIAA JOURNAL 59. no.6*: pp. 1990-2000.

[31] Masters, D. A., Taylor, N. J., Rendall, T. C. S., Allen, C. B., & Poole, D. J. (2017) Geometric comparison of aerofoil shape parameterization methods. *AIAA JOURNAL 55, no.5*: pp. 1575-1589.

[32] Kohar, C. P., Greve, L., Eller, T. K., Connolly, D. S., & Inal, K. (2021) A machine learning framework for accelerating the design process using CAE simulations: An application to finite element analysis in structural crashworthiness. *Comput. Methods Appl. Mech. Engrg. 385*: pp. 114008.

[33] Li, J., & Zhang, M. (2020) Efficient aerodynamic shape optimization with deep-learning-based geometric filtering. *AIAA JOURNAL 58, no.10*: pp. 4243-4259.

[34] Li, J., & Zhang, M. (2021) Data-based approach for wing shape design optimization. *Aerospace Science and Technology 112*: pp. 106639.

[35] Lye, K. O., Mishra, S., Ray, D., & Chandrashekar, P. (2021) Iterative surrogate model optimization (ISMO): An active learning algorithm for PDE constrained optimization with deep neural networks. *Comput. Methods Appl. Mech. Engrg. 374*: pp. 113575.

[36] Zhou, H., Xu, Q., Nie, Z., & Li, N. (2021) A study on using image-based machine learning methods to develop surrogate models of stamp formign simulations. *Journal of Manufacturing Science and Engineering 144*: pp. 021012.

[37] Bogoclu, C., Roos, D., & Nestorović, T. (2021) Local Latin hypercube refinement for multi-objective design uncertainty optimisation. *Applied Soft Computing*: pp. 107807.

[38] Chang, K., & Cheng, C. (2020) Learning to simulation and design for structural engineering. *In International Conference on Machine Learning*: pp. 1426-1436, PMLR.

[39] Ganapathy, M., Li, N., Lin, J., Abspoel, M., & Bhattacharjee, D. (2019) Experimental investigation of a new low-temperature hot stamping process for boron steels. *The International Journal of Advanced Manufacturing Technology 105*: pp. 669-682.

[40] Pongetti, J., Kipouros, T., Emmanuelli, M., Ahlfeld, R., & Shahpar, S. (2021) Using autoencoders and output consolidation to improved machine learning for turbomachinery applications. *Proceedings of the ASME 2021 Turbomachinery Technical Conference & Exposition*.